Turbulence Structure in Bubble Disengagement Zone: Role of Polymer Addition

R. B. Desai, R. V. Kolhatkar, and J. B. Joshi
Dept. of Chemical Technology, University of Bombay, Matunga, Bombay 400 019, India

V. V. Ranade and R. A. Mashelkar
National Chemical Lab, Pune 411 008, India

Experimental studies of turbulent stresses have been reported near the gas-liquid interface of a two-dimensional bubble column using a laser doppler anemometer. The breakage of bubble in this region results in extra turbulence and energy dissipation causing damage to the cells. The thickness of the region of high turbulence has been measured. The level of turbulence was reduced by the addition of drag reducing polyacrylamide polymer. A simple model has been proposed for the prediction of extra turbulence in the bubble breakage layer.

Sparged reactors are commonly used as bioreactors because of their simple construction and ease of operation. However, direct sparging is detrimental to many animal and insect cells even at mild conditions. Recent experiments have shown that the major damage to the cells is caused in the region where the bubble reaches the gas–liquid interface and disengages itself after it collapses into the free space (Cherry and Hulle, 1992). These reports suggest that cell death does not result from the shear that the cell experiences when the bubble is rising in the bulk itself. No measurements of the turbulent stresses have yet been reported for the region near the gas-liquid interface (bubble disengagement section) of the sparged reactors. This article reports such data. An attempt to understand the main issues involved has been made so that further research can be focused to develop quantitative models. The idea of using drag reducing polymers to reduce the turbulence levels near the interface has been proposed and tested for the first time.

Newitt et al. (1953) have discussed experimentally the physical processes accompanying the rupture of a bubble in the bubble disengagement zone (Figure 1). A thin liquid film forms between a quasi-hemispherical bubble and the interface (Figure 1a). This film thins by gravity and capillary forces until it reaches critical thickness and then the process of spontaneous rupture takes place (Figure 1b). After a bubble collapses, a cavity is formed at the interface (Figure 1c). The surrounding liquid rushes to fill this cavity. Finally a small droplet is formed at the tip of the jet (Figure 1f). All these events generate intense turbulence in the vicinity of the gas-liquid interface.

Experimental Studies

Measurements were made in a rectangular 2-D bubble column made up of Plexiglas (Figure 2a). The two walls of which were separated by a distance of 10 mm. The column width was 0.15 m. The sparger consisted of equally paced 23 hypodermic needles (gauge no. 26) in a row placed at the bottom of the column as shown in Figure 2a. Air was supplied by an oil free air compressor. The gas-flow rate was measured with a capillary meter. Experiments were conducted with water and an aqueous solution of polyacrylamide at a fixed concentration of 100 ppm. Polyacrylamide with a molecular weight of about 10^6 was procured from Union Carbide (Separan AP 30). Velocity measurements were made using a laser doppler anemometer (LDA). Ranade and Joshi (1990) provided pertinent details of LDA measurements.

Results and Discussion

Experimental results

Figures 3a and 3b show velocity histograms for the horizontal and vertical components, respectively. From Figure 3a it can be seen that a large peak exists with a mean close to zero. This is because the homogeneous regime prevailed in the range of superficial velocities covered in this work. This means that the gas holdup was practically uniform in the transverse direction and the internal liquid circulation was absent. From Figure 3a it can also be seen that two small peaks appear on either side of the zero mean. These occur because of the bubble motion. When a bubble rises in the neighborhood of the measurement point, an instantaneous horizontal component of liquid velocity is generated. This instantaneous velocity can be positive or negative, since the bubbles rise on either side of the measurement point. The

Correspondence concerning this article should be addressed to J. B. Joshi.

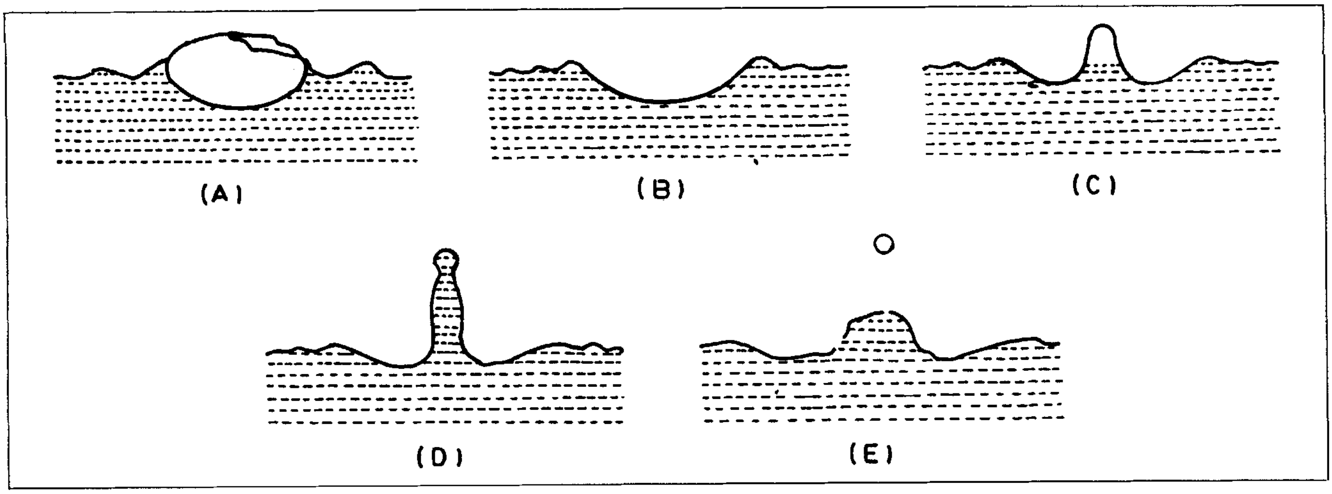

Figure 1. Bubble burst.

histogram for the vertical velocity (Figure 3b) is almost similar to that for the horizontal component except for an additional peak in the velocity range of 0.25 to 0.4 m/s. When the measurement point is inside the bubble or wake, the measured velocity corresponds to the bubble rise velocity. Thus, the additional peak corresponds to the bubble rise velocity. It may be pointed out that such a peak occurs only in the vertical velocity histogram. The mean of additional peak was found to be in the range of 0.25 to 0.35 m/s, which corresponds to the slip velocity of the bubbles.

For estimating the liquid-phase root mean square (rms) velocity, the central three peaks were included. The mean and rms measurements were made at ten equidistant locations in the horizontal direction and five locations in the vertical direction. Typical results of vertical and horizontal rms at two superficial gas velocities are shown in Figures 4a and 4b. Isotropic turbulence can be seen. For of variables covered in this work, the Kolmogorov length scale was 25–100 microns.

Velocity measurements were then carried out in the bubble disengagement region of the contactor. It was observed that the rms at the interface was 1.5 to 2 times higher than that in the bulk of the dispersion. However, the rms was found to decrease very sharply, as one moved, inside the bulk of the liquid. At a distance greater than 2 mm, rms was found to be practically independent of the distance from the interface. The variation of the turbulence intensity (shown as the product of the axial and radial rms, which can be considered approximately equal to Reynold's stress) with respect to distance is shown in Figure 5. It can be seen that at a V_G of 3.3 mm/s, the stresses are much higher at the interface, about seven times the value in the bulk. The extent of difference was found to decrease with an increase in the superficial gas velocity (V_G), as shown in Figure 5.

The effect of the presence of long chain polymer on Reynolds stresses is also shown in Figure 5. It can be seen that in the presence of 100 ppm polyacrylamide the level of interface stress decreases by a factor of two. This finding can have pragmatic implications in reducing the extent of cell death in bioreactors by addition of a small quantity of long chain polymer.

The value of rms in the vicinity of interface can be explained from the mechanism of the burst of a bubble at the top interface, as shown in Figure 1. This additional turbulence occurs in a small region equivalent to half the minor axis of the ellipsoidal bubble (Figure 1a), which is of the order of less than 2 mm for the air-water system. Secondly, the fractional gas holdup in the vicinity of the interface was found to be higher than that in the bulk. Therefore, the liquid-phase velocities get enhanced because of the reduction in the liquid holdup. Finally, the surface energy associated with the bubbles (equivalent to $2\sigma/d_B$) is released after the breakup of bubbles at the interface. This energy is dissipated by generating additional turbulence.

A simple model can be developed by assuming that all the surface energy gets dissipated in the top thin layer near the gas-liquid interface. Surface energy per bubble can be estimated as:

$$E_b = 2\sigma\pi d^2 \tag{1}$$

If we assume that the energy of all bubbles gets dissipated in layer of thickness proportional to the bubble diameter, we can write:

$$E_s = \left(\frac{12}{\alpha}\right)\left(\frac{1}{\epsilon_{LT}}\right)\left(\frac{\sigma V_G}{\rho_L d_B^2}\right) \tag{2}$$

where E_s is the rate of dissipation of surface energy and α is the proportional constant between the thickness of the top layer and the bubble diameter. Further, it has been assumed that the energy associated with the droplets (Figure 1e) is negligible.

The energy input rate in bubble columns is given by the following equation:

$$E = (\pi/4)D^2 V_G H(1-\epsilon_G)\rho_L g$$

The mass of the liquid is

$$M = (\pi/4)D^2 H(1-\epsilon_G)\rho_L$$

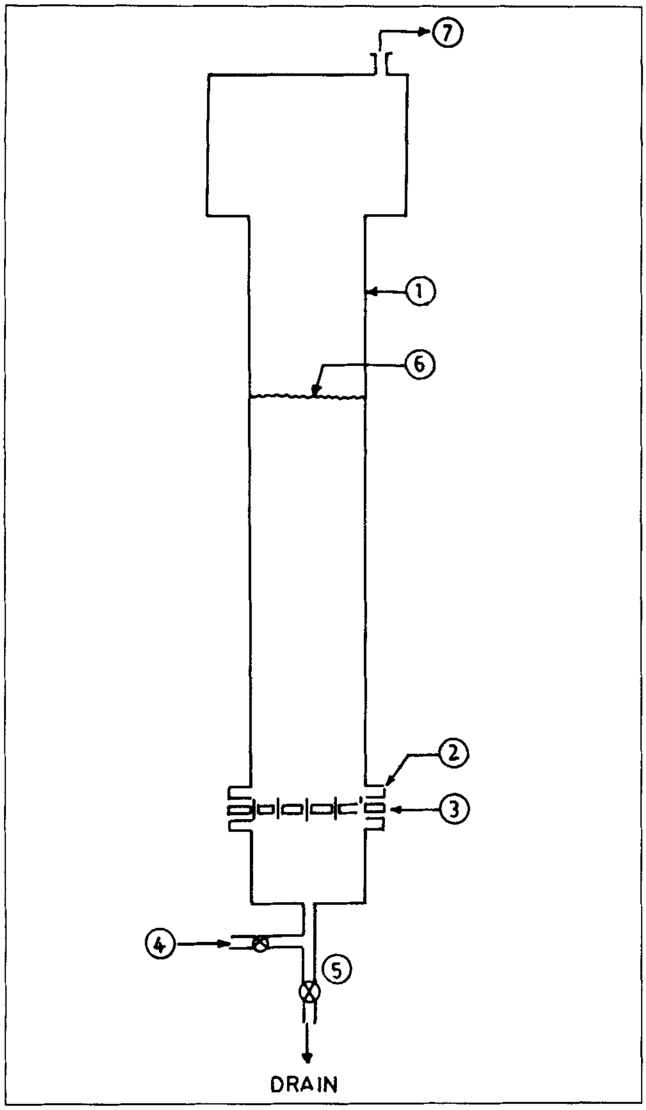

Figure 2. Bubble column (front view).

(1) 2-D bubble column; (2) flanges for sparger; (3) sparger plates with needles; (4) air inlet; (5) drain; (6) top gas-liquid interface; (7) air inlet.

Therefore, the energy dissipation rate E_B per unit mass is:

$$E_B = gV_G \tag{3}$$

Therefore, the total energy dissipation rate in the top region E_T can be written as:

$$E_T = E_b + E_s \tag{4}$$

If the scale of energy containing eddies is assumed to be the same in the bulk and the top region, the ratio of turbulence intensities at the interface to bulk can be written as:

$$\frac{u'_T}{u'_B} = \left(\frac{E_T}{E_B}\right)^{1/3} = \left[1 + \left(\frac{12}{\alpha}\right)\left(\frac{1}{\epsilon_{LT}}\right)\left(\frac{\sigma}{gd_B^2 \rho_L}\right)\right]^{1/3} \tag{5}$$

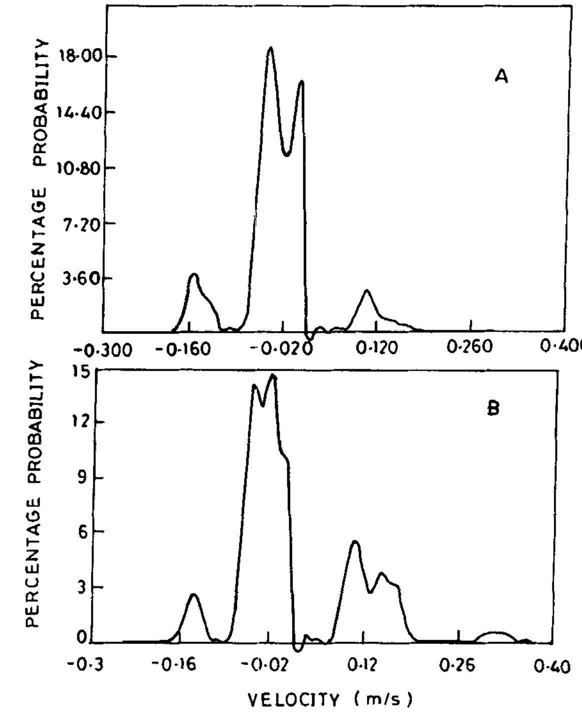

Figure 3. Velocity histogram.

(a) horizontal velocity component; (b) vertical velocity component.

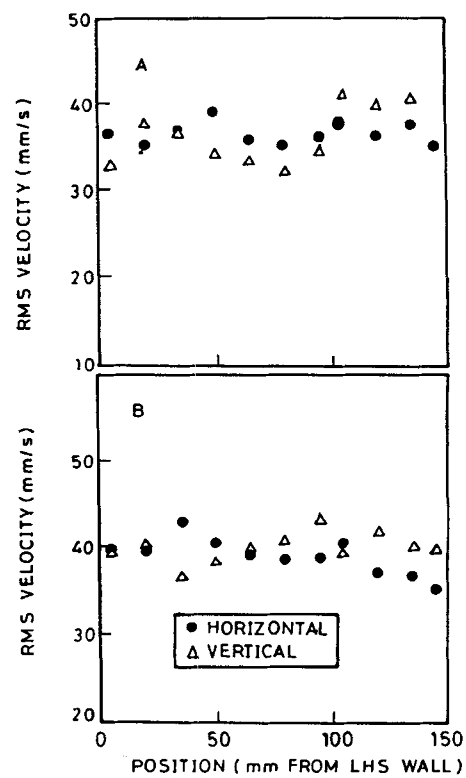

Figure 4. RMS velocity for horizontal and vertical velocity components.

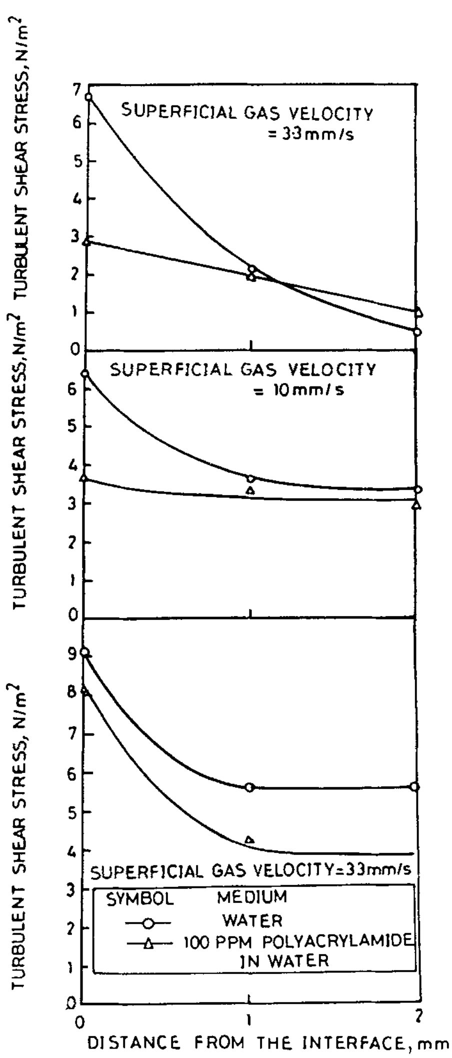

Figure 5. Behavior of shear stress near interface for water and 100 ppm PAA.

For air water system, the value of dimensionless parameter $\sigma/gd_B^2\rho_L$ is 0.8, if the bubble diameter is 3 mm. If we take α and $1/\epsilon_{LT}$ as unity, the ratio of u'_T to u'_B would be 1.5. Experimental data lend support to this value.

Effect of polymer addition

The fact that the addition of a polymer reduces turbulent stresses in the top region can be attributed to the following reasons. The bubble size in the presence of polyacrylamide (PAA) is higher than that in its absence (Ranade et al., 1978). Therefore, the surface energy associated with bubbles is less. Further, the gas holdup at the interface was found to be less in the presence of PAA. This is because of the enhanced rate of coalescence at the interface. The hydrodynamics depicted in Figure 1 shows strong extensional components. It is well-known that the polymer solution such as PAA are extension thickening as their extensional viscosity is covered. There is thus a strong possibility of retardation of motions (Mashelkar, 1973, 1984).

Conclusions

The velocity histograms obtained by the measurements using laser doppler anemometer clearly show the presence of bubbles. Further, the liquid-phase turbulence was found to be isotropic.

The liquid-phase rms velocity and Reynolds stress were found to be much higher at the top gas-liquid interface. The thickness of this region was found to be less than 2 mm.

The rms velocity and Reynolds stresses at the interface decreased substantially in the presence of long chain polymers. This finding has pragmatic indications, since the extent of cell damage in bioreactors having animal cells can be reduced by doing some polymer addition.

Acknowledgment

This work was supported by a project entitled "Development of Column Type Bioreactors" From the Department of Biotechnology, Government of India.

Notation

d_B = bubble diameter
E_b = surface energy per bubble
E_B = energy dissipation rate in bulk
E_T = total energy dissipation rate in interface region
u'_T/u'_B = ratio of turbulence intensities of interface to bulk
V_G = superficial gas velocity
ϵ_{LT} = liquid holdup in top layer
ϵ_{LB} = liquid holdup in bulk
σ = surface tension

Literature Cited

Cherry, R. S., and C. T. Hulle, "Cell Death in Thin Films of Bursting Bubbles," *Biotechnol. Prog.*, **8**, 11 (1992).

Newitt, M. D., N. Dombrowski, and F. H. Knelman, "Liquid Entrainment: 1. The Mechanism of Drop Formation from Gas or Vapour Bubbles," *Trans. Inst. Chem. Engrs.*, **32**, 244 (1954).

Ranade, V. V., and J. B. Joshi, "Flow Generated by Disc Turbine," *Chem. Eng. Res. Dev.*, **68**, 19 (1990).

Ranade, V. R., and J. J. Ulbrecht, "Influence of Polymer Additives on the Gas-Liquid Mass Transfer in Stirred Tanks," *AIChE J.*, **24**, 796 (1978).

Mashelkar, R. A., "Drag Reduction in External Rotational Flows," *AIChE J.*, **19**, 382 (1973).

Mashelkar, R. A., "Anomalous Convective Diffusion in Films of Polymeric Solutions," *AIChE J.*, **30**, 353 (1984).

Manuscript received May 5, 1993, and revision received June 27, 1994.